Journal of the Meteorological Society of Japan, Vol. 88, No. 2, pp. 123–134, 2010.
DOI:10.2151/jmsj.2010-202

Development of a Compact and Sensitive Electrostatic Radon-222 Measuring System for Use in Atmospheric Observation

Akira WADA

Meteorological College, Kashiwa, Japan

Shohei MURAYAMA, Hiroaki KONDO

National Institute of Advanced Industrial Science and Technology (AIST), Tsukuba, Japan

Hidekazu MATSUEDA, Yousuke SAWA

Meteorological Research Institute, Tsukuba, Japan

and

Kazuhiro TSUBOI

Japan Meteorological Agency, Tokyo, Japan

(Manuscript received 4 August 2009, in final form 9 December 2009)

Abstract

A new automated ^{222}Rn measuring system suitable for a wide range of atmospheric observations has been developed. This system comprises a ^{222}Rn analyzer and an air-sampling unit, along with a pump, drying equipment, and a filter. The operation of this ^{222}Rn analyzer is based on an electrostatic collection method involving the use of a PIN photodiode to separately detect α particles emitted from ^{218}Po and ^{214}Po released from the decay of ^{222}Rn in a hemispheric air-sample chamber. The response of the ^{222}Rn analyzer with respect to the applied voltage, chamber volume size, and sample flow rate is investigated to determine the appropriate measuring conditions. With this instrument, the detection limits have improved to 0.16–0.20 Bq m^{-3} for 1 h. The new ^{222}Rn analyzer shows several technical advancements over the previous electrostatic collection methods, such as an improved detection limit, higher sensitivity, higher time-resolution analysis, and longer life. During the preliminary observational test, the ^{222}Rn measuring system was able to detect the diurnal cycle in ^{222}Rn resulting from the mixing of rapid vertical air in the surface boundary layer. At the Minamitorishima station located far from the continent, very small ^{222}Rn peaks were clearly detected when long-range transport of polluted air masses from the Asian continent was observed at the station. We demonstrate that our compact ^{222}Rn measuring system has the potential to be widely used for high time-resolution measurements of low-level ^{222}Rn.

1. Introduction

Radon-222 (^{222}Rn) is a naturally occurring radioactive noble gas with a half life of 3.824 days. It is mainly emitted from ice-free land surfaces by the decay of Radium-226 (^{226}Ra) in mineral soil. Its

Corresponding author: Akira Wada, Meteorological College, 7-4-81 Asahicho, Kashiwa, Chiba 277-0852, Japan.
E-mail: awada@mc-jma.go.jp

continental flux to the atmosphere is estimated to be approximately 1 atom cm^{-2} s^{-1}, although this value varies in time and space (Conen and Robertson 2002). ^{222}Rn is also emitted from dissolved ^{226}Ra in the ocean, but the total oceanic flux is approximately two orders of magnitude less than the total continental flux (Wilkening and Clements 1975). Thus, due to its relatively well-known sources and radioactive decay time, atmospheric ^{222}Rn measurements can be used to trace continental air masses on local, regional, and intercontinental scales (Zahorowski et al. 2004). Consequently, observed ^{222}Rn data have been used for validating atmospheric transport model processes (e.g., Li and Chang 1996; Stockwell and Chipperfield 1999; Chevilland et al. 2002; Taguchi et al. 2002; Gupta et al. 2004; Josse et al. 2004) and for model intercomparison experiments (e.g., Jacob et al. 1997; Rasch et al. 2000).

Atmospheric ^{222}Rn observations have also been used to obtain emission inventories of various trace gases over the continental regions. Schmidt et al. (1996) and Levin et al. (1999) showed that atmospheric ^{222}Rn can be used to estimate methane flux density in Western Europe. Similar methodologies were applied to evaluate emissions of CO_2 (Schmidt et al. 2003), N_2O (Schmidt et al. 2001), and CFCs (Biraud et al. 2000). In another approach, Trumbore et al. (1990) estimated the rates of ecosystem gas exchange between the air above and below the soil surface and these between the air inside and above the canopy layer in the Amazon rain forest, using ^{222}Rn concentration measurements in the soil and the atmosphere. Martens et al. (2004) reported on a method for estimating the net ecosystem exchange (NEE) of CO_2 using measurements of atmospheric ^{222}Rn accumulation in the Brazilian rain forest during night time. A similar method has also been applied to the estimation of N_2O flux from soil (Conen et al. 2002).

In order to measure atmospheric ^{222}Rn, four different methods have been used: (1) an ionization chamber (Budnits 1974), (2) a scintillation cell (Lucas 1957), (3) a two-filter method (Thomas and LeClare 1970; Whittlestone 1985; Zahorowski and Whittlestone 1996; Tokonami et al. 1996; Whittlestone and Zahorowski 1998; Brunke et al. 2002), and (4) an electrostatic collection method (Dula and Dalu 1971; Wrenn et al. 1975; Iida et al. 1991, 1996; Ui et al. 1998; Iimoto et al. 1998). The first two methods have low sensitivities and are hence not used extensively; the last two methods, however, have often been applied in various kinds of atmospheric chemistry studies.

The two-filter method is used to measure the low-level concentrations of atmospheric ^{222}Rn in remote areas that are far removed from continents. The sensitivity of this method is increased by collecting large volumes of sample air (Whittlestone and Zahorowski 1998); this requires an extremely large sample chamber with a volume of approximately a few cubic meters and powerful pump with a high air flow rate of approximately 200 L min^{-1} (Whittlestone and Zahorowski 1998). Such a large chamber is not suitable for measurements at small observatories. Furthermore, a high air flow rate makes it difficult to efficiently dehumidify sample air to prevent water condensation in the sample chamber under humid climate conditions that exist in temperate and subtropical regions. On the other hand, the electrostatic collection method, with a slight degradation in the detection limit when compared to that of the two-filter method, has the advantage of requiring only a relatively smaller sample chamber with a volume of approximately 10–70 L and a smaller air pump with a flow rate of approximately a few liters per minute; this is because it can effectively collect ^{222}Rn progenies by applying a high negative voltage on the detector (Iida et al. 1991). These advantages make it possible to efficiently dehumidify sample air and reduce the size of the instrument, and reduce the electric power consumption during operation. In addition, the compactness of the system allows for higher time-resolution measurements because of rapid exchange of air in the sample chamber.

In the electrostatic collection method, the type of detector used for counting α particles plays an important role. A zinc sulfide–silver (ZnS (Ag)) scintillator is easy to handle and highly sensitive (Iida et al. 1991), but it cannot detect ^{222}Rn progenies separately due to the lower detecting resolution of α particle energy. On the other hand, a silicon photodiode detector can provide a higher resolution spectrum of α particle energy. Ui et al. (1998) reported that a PIN Si photodiode is useful for low-level ^{222}Rn measurements, but a relatively large volume of collecting chamber is required to obtain a high sensitivity and low background noise. The PIN Si photodiode is used as an α particle detector not for ^{222}Rn but for the ^{220}Rn analyzer (Iimoto et al. 1998). Therefore, at the present time, there is a need to develop a more compact ^{222}Rn measuring system with a high sensitivity and a higher time-

resolution that can be easily and widely used in atmospheric chemistry studies, particularly at remote locations.

We have developed such a system by employing the electrostatic collection method and by using the PIN photodiode detector. In this paper, we provide a detailed description of the technical and practical aspects of the new ^{222}Rn measuring system and draw a comparison between the performances of the developed system and other ^{222}Rn measuring systems that employ the same electrostatic collection method. We also report some of the preliminary measurement results that demonstrate the capability of the system when operated under two different environments.

2. Instrumentation

2.1 ^{222}Rn analyzer

Figure 1 shows a schematic diagram of the electrostatic ^{222}Rn measuring system in this study. This system consists of two main parts: a ^{222}Rn analyzer and an air sampling unit. The ^{222}Rn atoms in the sample air inside the chamber in the analyzer unit, undergo α decay by emitting α particles and are transformed into ^{218}Po ions. The ^{218}Po ions are then collected electrostatically on a negative electrode since most of the ^{218}Po ions are positively charged (Dua et al. 1983). The ^{218}Po ions and its progeny ^{214}Po ions collected on the electrode decay by emitting α particles, which are then counted by the PIN photodiode detector. In order to make this electrostatic method effective, the ^{222}Rn analyzer is designed to consist of a hemispherical chamber equipped with a PIN photodiode on a charge amplifier, a spectroscopy amplifier, a multichannel analyzer (MCA), and a PC for data collection and system control.

Three stainless steel chambers with internal volumes of 6 L, 16.8 L, and 32 L are prepared to test the sensitivity of the detection limit to the chamber size. The internal surface of each chamber is treated by buffing in order to minimize the emissions of ^{222}Rn and ^{220}Rn from the internal wall. Ui et al. (1998) pointed out that such treatment is essential for improving the detection limit of ^{222}Rn. The shape of each chamber is hemispheric, because Iida et al. (1991), theoretically calculated the electric force fields inside the chamber when a detector is attached to the center of the chamber at the bottom and reported that this is the most effective shape for collecting ^{222}Rn progeny.

The PIN photodiode used in our instrument is a large-area Si PIN photodiode (S3204-06-SPL, Hamamatsu Photonics K.K.) having length, width, and thickness of 18 mm, 18 mm, and 0.5 mm, respectively. The photodiode is covered with a ceramic frame in order to avoid rusting by water vapor. In order to electrostatically collect the ^{218}Po

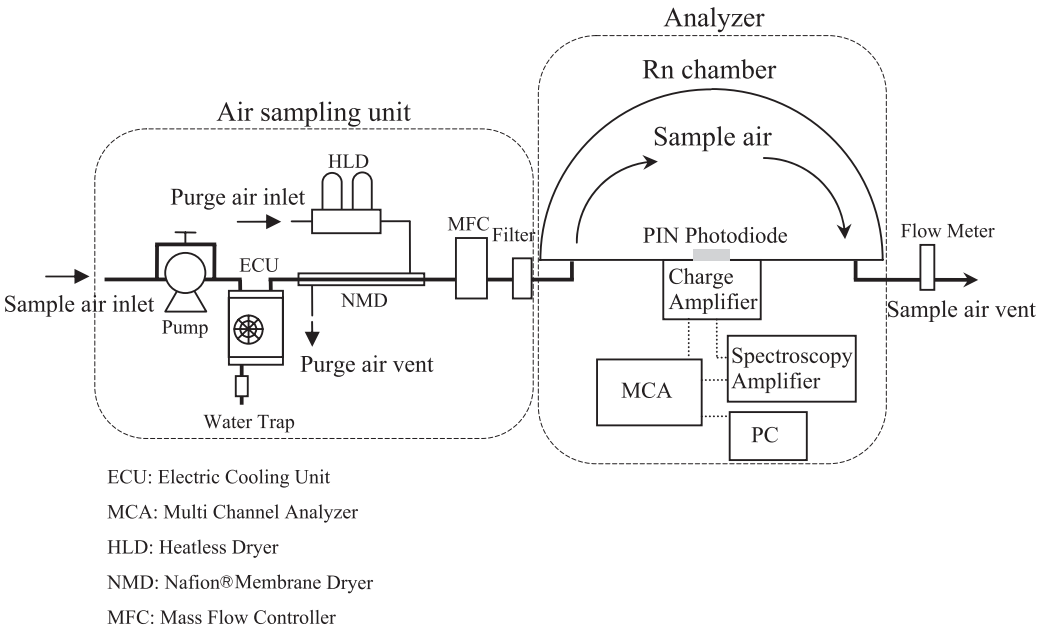

Fig. 1. Schematic diagram of the atmospheric ^{222}Rn measuring system.

ions on the PIN photodiode detector, a high negative voltage (−2500 to −3000 V) is applied on the cathode side (N layer) of the photodiode. If a voltage of −3000 V is applied on the cathode side, then a slightly lower negative voltage of −2850 V is applied on the anode side (P layer) to keep the voltage difference between the P and N layers at 150 V, because the PIN photodiode used in this study cannot be applied at a voltage differences of more than 150 V. The ^{218}Po ions collected on the PIN photodiode emit α particles, thereby releasing free electrons from the silicon atoms in the photodiode. The ^{214}Po ions produced from ^{218}Po further undergo α decay by emitting α particles, producing more free electrons due to higher energy of the α particles emitted from ^{214}Po when compared to the energy of that α particles emitted from ^{218}Po. This difference in the amount of electrons generated can be detected by the PIN photodiode on the basis of the signals received from ^{218}Po and ^{214}Po.

Since the signals detected by the photodiode are faint, they are amplified eight-fold in the charge amplifier (Model 5537, Clear-Pulse) that is attached under the ^{222}Rn chamber. Furthermore, these signals are sent to the spectroscopy amplifier (Model 4419, Clear-Pulse) and are further amplified 10-fold. These amplified signals of the α particles with energies in the range of 10 MeV are converted to corresponding voltages ranging from 0 to 10 V as analog output data. These analog data are sent to the MCA with a 16-bit resolution to be converted to digital data, which are allocated from 1 to 1024 channels to obtain the α spectrum of the ^{222}Rn progenies.

Data from these 1024 channels are stored on a hard disk drive of the PC. A new operating software has been developed to monitor the spectral data, as well as to control the conditions of the instrument, such as applied voltage and interval time during measurement.

2.2 *Air sampling unit*

The schematic diagram of the air sampling unit connected to the ^{222}Rn analyzer is shown in Fig. 1. Sample air is drawn in by a diaphragm pump (ANE022, KNF) and then introduced into a drying system with an electric cooling unit (DH-109, KELK Ltd.) and a nafion® membrane dryer (MD-110-72P, Perma Pure Ltd.). Since water vapor affects the collection efficiency of ^{218}Po ions due to the neutralization effect (Busigin et al. 1981; Kotrappa et al. 1981; Dua et al. 1983; Chu and Hopke 1988; Ui et al. 1998; Iimoto et al. 1998), the dew point of the sample air is kept at approximately −2°C in the drying system. The flow rate of dry air is maintained within a range of 1–5 L min^{-1} by using a mass flow controller. Before the introduction of dry air into the ^{222}Rn chamber, a membrane filter (0.8 μm) is used to remove the decay products of ^{222}Rn generated in the air sampling unit.

3. Instrument characterization

3.1 *Performance of the ^{222}Rn detector*

Figure 2 shows an example of an α spectrum of ^{222}Rn progenies of indoor air measured by the ^{222}Rn analyzer for 24 hours at a flow rate of 5 L min^{-1}. In this spectrum, two dominant peaks around 594 and 762 MCA channels are clearly found. These peaks correspond to ^{218}Po (6.003 MeV) and ^{214}Po (7.687 MeV), respectively, and are clearly resolved. As described above, the resolved ^{218}Po peak enables us to make measurements with higher time resolution for several 10's of minutes because, although ^{218}Po decays to ^{214}Pb with a half life of only 3.10 minutes, ^{214}Po arrives on the scene from decays of ^{214}Pb and ^{214}Bi with a relatively longer half lives of 26.8 and 19.9 min, respectively. Although the ^{218}Po peak overlaps a ^{212}Bi peak (6.051 MeV) originating from the ^{220}Rn decay with the emission of α particles of similar energy levels, it could be theoretically calculated to eliminate the interference of ^{212}Bi peak using counts of ^{212}Po peak, which is separately detected in our α spectrum. Thus, counts from ^{212}Bi included in the ^{218}Po peak are estimated to be negligible.

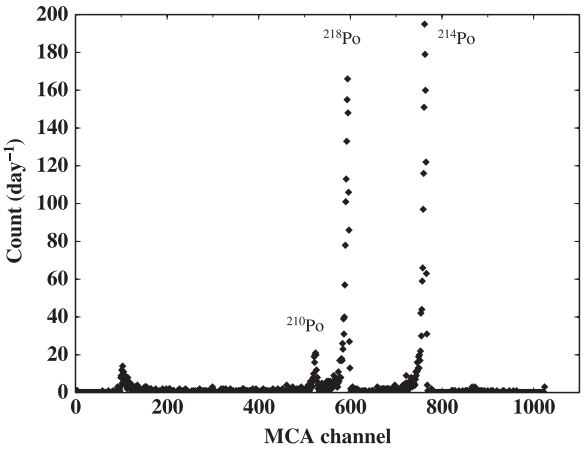

Fig. 2. A typical α spectrum from the progenies of ^{222}Rn. Signals less than 100 MCA channel are not shown.

In the spectrum, a smaller peak appears around the 525 MCA channel, which corresponds to the ^{210}Po peak (5.304 MeV) (Fig. 2). Since ^{210}Po is derived from ^{210}Pb (half life; 22.3 years) deposited on the photodiode detector, its peak will gradually increase. Fortunately, the ^{210}Po peak is completely separated from the ^{218}Po peak, indicating no interference of the ^{210}Po increase with the ^{222}Rn measurements. Although our measuring instrument has been in use for more than three years, the ^{210}Po peak is still completely separated from the ^{218}Po peak; this indicates that the detector in our system can be used for a long time without overestimating the ^{222}Rn concentration due to the inclusion of ^{210}Po counts. Other types of detectors that do not have the resolving power to separate out the two peaks have to be removed for a few years to eliminate the overestimation effect.

As described above, the MCA channel is adjusted by the amplifier to approximately correspond to the α particle energy from the ^{222}Rn progenies. To confirm the α particle energy from ^{218}Po and ^{214}Po, we examined the decay curves of the two major peaks corresponding to ^{218}Po and ^{214}Po in the α spectrum (Fig. 3). The ^{222}Rn chamber with a 32-L volume was filled with indoor air and its inlet and outlet were then closed to regularly monitor the count attenuations of the two peaks for approximately 10 days. As shown in Fig. 3, the counts associated with both peaks decrease exponentially with time. The exponential decay curves show attenuation constants of 0.1828 ± 0.0027 day^{-1} and 0.1841 ± 0.0033 day^{-1} for the ^{218}Po and ^{214}Po peaks, respectively, with no statistically significant difference at 95% confidence interval. These attenuation constants are in good agreement (statistically significant at 95% confidence interval) with the decay constant of ^{222}Rn (0.1813 day^{-1}). A similar result was also obtained in the case of a 16.8-L chamber. On the basis of these results, it is concluded that the two major peaks were in fact associated with the α particles from the ^{222}Rn progenies.

By using the results from Ui et al. (1998) and Iimoto et al. (1998) as a point of reference for changes in the counting rate with applied voltage, we also conducted an investigation to determine the optimal applied voltage on the photodiode for our ^{222}Rn analyzer as follows. The 16.8-L chamber was filled with dehumidified sample air and then its inlet and outlet were closed to monitor the decay of the ^{218}Po counts with time. At first, a voltage of -3000 V was applied on the photodiode until a decay trend curve was established. Next, the applied voltage was changed stepwise from -3000 V to -1000 V at intervals of 250 V to obtain a relationship between applied voltage and ^{218}Po counts because the ^{218}Po count varies as a function of the applied voltage. The ^{218}Po counts at each applied voltage were normalized by those obtained at -3000 V. Figure 4 shows the change in the relative ^{218}Po count when using the 16.8-L chamber as a function of the applied voltage. The relative count

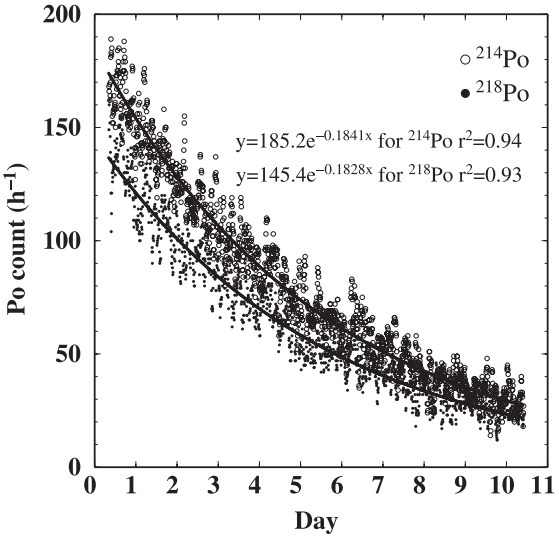

Fig. 3. Decay curves of the ^{222}Rn progenies. The solid lines represent the e-fold regression curves of ^{218}Po and ^{214}Po.

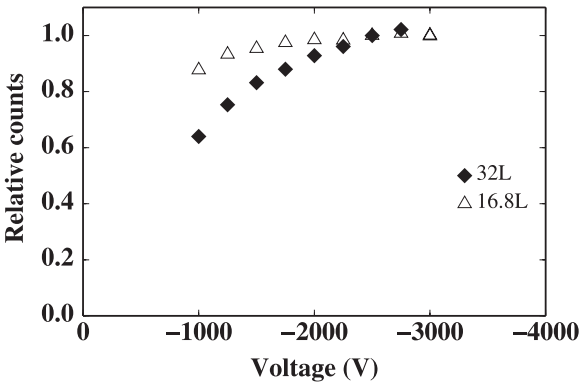

Fig. 4. Relative counts as a function of applied voltage for ^{218}Po. The counts at each applied voltage normalized by those at -3000 V and -2500 V are shown for the 16.8-L and 32-L chambers.

remains relatively constant as the voltage is changed from −3000 V to −2000 V, with a gradual decrease until the lowest value is recorded at −1000 V. A similar behavior of the PIN photodiode detector was also reported by Iimoto et al. (1998). These results indicate that the collection efficiency of ^{218}Po in the 16.8-L chamber became saturated below the voltage value of −2000 V.

A similar experiment was also conducted by using the 32-L chamber. The result is also shown in Fig. 4, where the ^{218}Po counts relative to those obtained at −2500 V are displayed. A similar pattern as before (using the 16.8-L chamber) is observed in Fig. 4, with the relative count increasing from −1000 V to −2500 V but not plateauing, as was the case in the 16.8-L chamber; this points to the requirement of a voltage value less than −2500 V for a higher collection efficiency with this volume size. However, when the applied voltage was set to −3000 V, the electric noise increased significantly for the entire range of the α energy level, and therefore, interfering with the detection limit. A similar problem was also reported by Ui et al. (1998). Considering the tradeoff between the noise effect and the collection efficiency, a voltage around −2500 V is deemed appropriate for the ^{222}Rn analyzer that uses the 32-L chamber. Thus, the optimal applied voltage used here was determined to be −3000 V for the 16.8-L chamber and −2500 V for the 32-L chamber.

3.2 *Measuring conditions of the chamber*

In order to select appropriate measuring conditions for the various kinds of field observations, we investigated the response of our ^{222}Rn analyzer as a function of the chamber volume size. Figure 5 shows the relative counting rates for three different chamber volumes of 6 L, 16.8 L, and 32 L. The relative counting rates were obtained for the dry natural atmospheric sample that was introduced simultaneously into the three chambers. It is clearly shown that the relative count rate increases linearly with an increase in the chamber volume, indicating that the count rate is linearly proportional to the amount of ^{222}Rn in the chamber. This empirical relation is useful in normalizing the amount of ^{222}Rn detected as a function of the volume of the chamber used.

In order to evaluate the time resolution for our ^{222}Rn analyzer, the gas exchange time as a function of flow rate was determined for the 32-L and 16.8-L chambers. The results are shown in Fig. 6. The gas

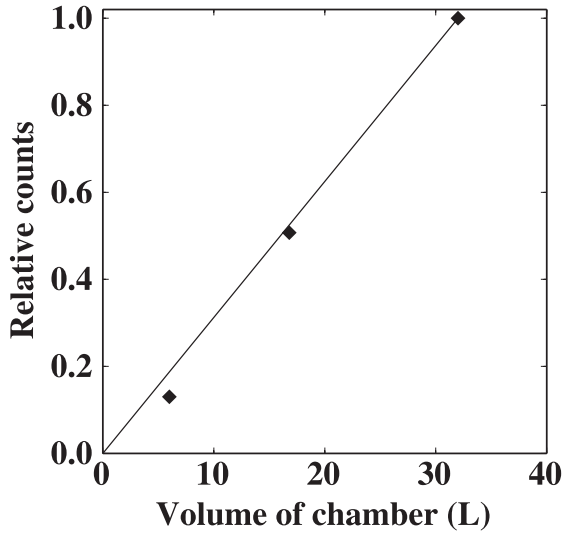

Fig. 5. Correlation between the relative count rate and chamber volume size. The plotted counts are normalized by the counts measured using the 32-L chamber. The solid line represents a linear regression with the intercept at zero.

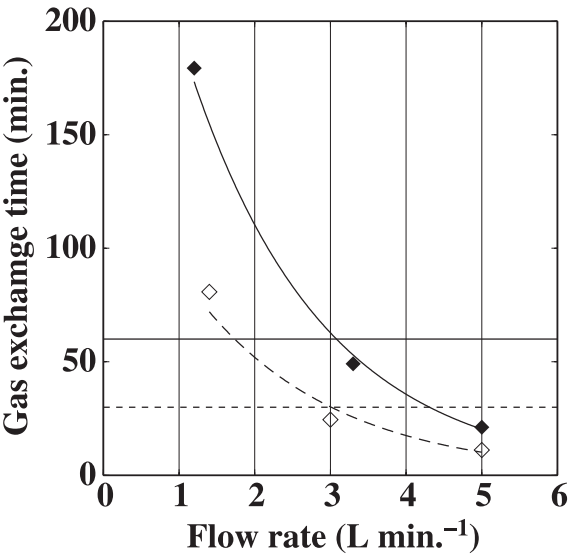

Fig. 6. Flow rate as a function of the gas exchange time for the 16.8-L and 32-L chambers. The solid squares and open diamonds represent the gas exchange time for the 32-L and 16.8-L chambers, respectively. The solid curve and dashed curve represent the e-fold regression curves. The horizontal solid line and the horizontal dotted line represent the 60-minute and 30-minute gas exchange times, respectively.

exchange time is defined as the time when 90% of the sample air in the chamber is exchanged. Two standard CO_2 gases with different concentrations were introduced into each chamber sequentially, and the changes in the concentration were measured by using a CO_2 analyzer (LI6262, LI-COR). The results in Fig. 6 indicate that the sampling interval for the 16.8-L chamber is 30 min at a flow rate of 3.0 L min^{-1} and 1 h at the same flow rate for the 32-L chamber. This result shows clearly that the gas exchange time depends significantly on the sample flow rate and is critical for determining the time resolution for the ^{222}Rn analyzer.

3.3 Calibration and counting efficiency

The ^{222}Rn analyzers with chamber volumes of 16.8 L and 32 L were calibrated by employing an ionization chamber method developed at Nagoya University (Iida et al. 1991). Calibration results such as the calibration factor, detection limit, and background counts are summarized in Table 1.

The calibration factor, defined as the ratio of the counting rate to the ^{222}Rn concentration, is determined from ^{218}Po counts to be 19.6 and 31.8 counts h^{-1} $(Bq\ m^{-3})^{-1}$ for the 16.8-L and 32-L chambers, respectively. This calibration factor depends on the chamber volume size because more ^{218}Po ions are produced in a larger chamber and thus increase the count.

The counting efficiency calculated from the calibration factor is defined as a percentage of the detected ^{218}Po ions to the total ^{218}Po emanated from ^{222}Rn in the chamber. For our system, the counting efficiencies are 0.32 and 0.27 for the 16.8-L and the 32-L chambers, respectively. One factor reducing the counting efficiency is the electrostatic collecting efficiency, which is defined as a percentage of the collected ^{218}Po ions on the electrode to the total ^{218}Po produced in the chamber. Since Hopke (1989) reported that 88% of ^{218}Po emanated from ^{222}Rn carried a positive charge, the counting efficiency is reduced by at least 12%. Another factor is the α counting efficiency for detecting α particles of the ^{218}Po ions collected on the surface of the photodiode detector. Since the α counting efficiency largely depends on the geometric shape of the photodiode, our flat photodiode can only detect less than 50% of the α particles emitted isotropically from the Po ions. Therefore, the theoretical maximum of the counting efficiency is estimated to be 0.44 from both of the positively-charged ^{218}Po to the total of ^{218}Po (88%) and the geometric effect (50%). Since the counting efficiency of 0.32 for 16.8-L chamber is calculated from the calibration factor, approximately 73% of the ^{218}Po ions from ^{222}Rn in sample air are counted by our new ^{222}Rn analyzer and are compared to the theoretical maximum value. The remaining 27% is lost due to insufficient collection related to the applied voltage, humidity of the sample air, and the probability of neutralization of the ^{218}Po ions.

Background counts are measured as ^{218}Po counts when aged air with no ^{222}Rn content is continuously introduced into the chamber from a high-pressure cylinder. The background counts for the 16.8-L and 32-L chambers are determined to be 0.06 and 0.38 counts h^{-1}, respectively. This difference between the two chambers suggests that the background counts are largely influenced by the emissions of ^{222}Rn or ^{220}Rn from the internal walls of the chamber. These background counts are recalculated to be approximately 0.003–0.01 Bq m^{-3} converted as the ^{222}Rn concentration, based on the calibration factors as described above.

Table 1. Comparison of some salient characteristics among several ^{222}Rn measuring instruments employing the electric collection method.

	This work		Ui et al. (1998)	Iida et al. (1996)
Detector	PIN photodiode		PIN photodiode	ZnS(Ag)
Flow rate of sample air (L $min.^{-1}$)	3.0	3.0	3.8	1
Chamber volume (L)	32	16.8	68.7	16.8
Calibration factor (counts $h^{-1}(Bq\ m^{-3})^{-1}$)	31.8	19.6	22.5†	17.8
Detection limit* (Bq m^{-3})	0.16	0.20	0.65†	0.42**
Average background counts (h)	0.38	0.06	0.56†	5.2

* Detection limit was calculated for 1 hour as defined by Currie (1968).

** Value recalculated from the original data in Iida et al. (1996) using the detection limit equation of Currie (1968).

† Value obtained after conversion from the unit used in original paper.

3.4 *Comparison of our system with other similar systems*

Table 1 shows a comparison of the characteristics of our instrument with those of the other two ^{222}Rn measuring systems that employ same electrostatic collection method. Some of the data from other studies have been converted into the units used in this paper for comparison purposes. Compared with the measuring system used by Ui et al. (1998), which has a photodiode detector similar to that has in our study, the calibration factor of our system with the 32-L chamber is approximately 40% higher, even though the chamber volume is approximately two times smaller. This higher sensitivity is caused mainly by the more effective collection efficiency of the ^{218}Po ions on the detector most likely due to the hemispheric shape of our chamber, as suggested by Iida et al. (1991). In addition, the detection limit of our system with the 32-L chamber is improved by a factor of four. This improvement is based on the lowest background counting in our system (see Table 1), although the chamber volumes are different from each other. Another factor contributing to the improved detection limit is a relatively small variation in the low-level counting (background) this results in a lower counting error of the background measurement (Currie 1968) and thus makes our ^{222}Rn analyzer more stable.

When compared to the measuring system of Iida et al. (1996), which has a different detector that comprises a ZnS (Ag) scintillator, the detection limit of our system with the 16.8-L chamber is better by about a factor of two. This improvement results from the fact that the average background count of our instrument is lower than that of the other by approximately a factor of two (Table 1). This reduced count is caused mainly by the absence of interference of the ^{210}Pb accumulation on the detector, as stated above. It can also be attributed to the buffing of the internal chamber walls in our system to minimize the emission of background α particles, whereas the aluminum chamber used by Iida et al. (1996) has not been subjected to any treatment. In addition, the calibration factor of our system with the 16.8-L chamber is slightly higher. The most significant advantage of our photodiode detector is that it provides a higher resolution spectrum of the α particle energy in order to resolve different ^{222}Rn progenies; this resolving power is not available in the ZnS (Ag) scintillator. It leads to improved time resolution by shortening the measuring interval and avoiding the interference of ^{210}Pb accumulation on the detector for long-term use, as discussed above. For these reasons, our system incorporates several new advancements in the electrostatic collection method for detecting ^{222}Rn. We can optimize the measurement condition in the field by suitably adjusting the chamber volume size and sample air flow rate.

4. Application for field observation

4.1 *Field observation at MRI in Tsukuba*

Preliminary observations using our instrument with a 16.8-L chamber were made on the meteorological observation tower (height: 213 m) located at the Meteorological Research Institute (MRI) in Tsukuba (36.1°N, 140.1°E, 26 m asl), approximately 50 km northeast of Tokyo, Japan. Figure 7 shows a time series of the ^{222}Rn concentration observed every 30 min at 1.5-m and 100-m levels from November 20 to November 24 in 2006. The ^{222}Rn concentration at 1.5 m shows a prominent diurnal cycle with a nighttime increase for two consecutive nights from November 21 to November 23. A corresponding increase was also observed at 100 m during the nighttime from November 22 to

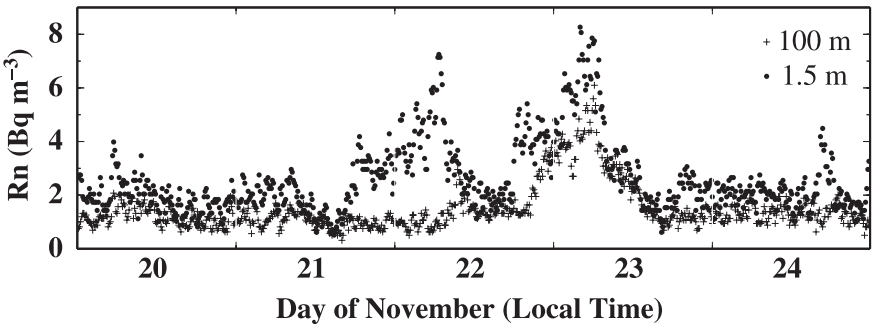

Fig. 7. Time series of half-hourly atmospheric ^{222}Rn concentration observed at Tsukuba in 2006.

November 23, but not from November 21 to November 22. This vertical difference observed during November 21 to November 22 was caused by the formation of a shallow inversion layer near the ground, a condition confirmed by a steep temperature gradient clearly revealed in the microwave temperature profiler data (not shown). A different situation with no clear diurnal cycle was observed on November 20 and November 21. During this period, it was cloudy or rainy and relatively windy, indicating no formation of a distinct inversion structure during the nighttime. These observational measurements show that the diurnal variation pattern of the atmospheric ^{222}Rn concentration is well associated with meteorological conditions within the surface boundary layer. Figure 7 convincingly shows that our measuring system can capture short-term variations in atmospheric ^{222}Rn over land.

This result demonstrates that our measuring system is useful for measuring rapid variations in ^{222}Rn concentration because of the instrument's high time resolution.

4.2 *Observation at the remote site of Minamitorishima*

Another preliminary ^{222}Rn observation was made at a remote coral island station of Minamitorishima (24.3°N, 154.0°E, 9 m asl) in the western North Pacific, approximately 2000 km southeast of Tokyo (Wada et al. 2007). Air samples were collected from the top of the observatory building by using a diaphragm pump and forced into the ^{222}Rn analyzer with the 32-L chamber at a flow rate of 3.0 L min^{-1}.

Figure 8 shows a time series of the hourly ^{222}Rn concentration, together with carbon monoxide (CO) mixing ratio simultaneously observed at Minamitorishima from September to December, 2007. Details of the CO measuring method are reported elsewhere (Wada et al. 2007). Throughout the observational period of time, the influence of the local source from this island is not significant for atmospheric ^{222}Rn measurements because this island is very small.

In mid-November, no measurements of ^{222}Rn and CO were carried out because of the maintenance work carried out on the air sampling system. In December, some distinct large peaks with ^{222}Rn concentrations of more than 0.8 Bq m^{-3} can be seen in Fig. 8. It is also shown that the overall variation in the ^{222}Rn measurements corresponds well with the observed variation in CO. On December 21, for example, the significant increase in ^{222}Rn of up to 1.8 Bq m^{-3} is associated with an enhanced CO peak. Sawa et al. (2007) have shown that higher CO mixing ratios observed at this site indicate long-range transport of continental air pollution from Asia. Thus, the close relation between ^{222}Rn and CO shows that increased ^{222}Rn peaks detected by our measuring system can capture the signal of continental air masses passing over this

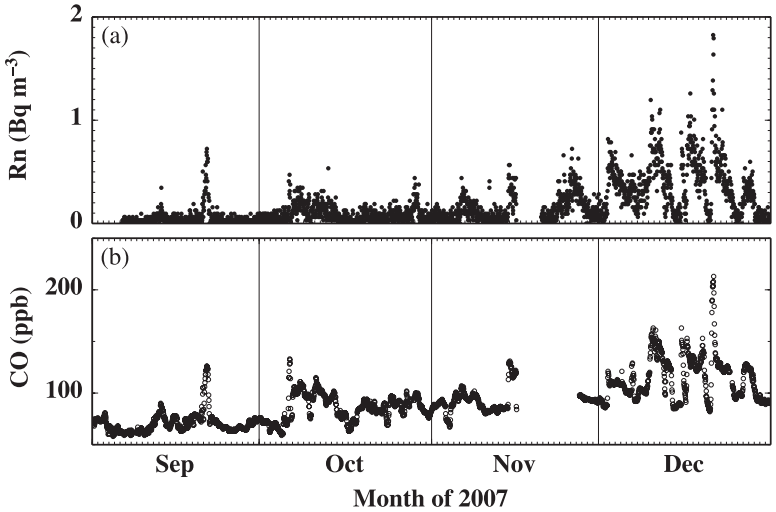

Fig. 8. Time series of the hourly concentrations of ^{222}Rn and CO observed at Minamitorishima from September to December, 2007.

remote site. We also find that all of the ^{222}Rn peaks in December were associated with rapid changes in wind speed and direction caused by the passage of cold fronts over the Minamitorishima station. Detailed mechanism for such frontal transport in the western North Pacific region was examined using a 3-D transport model by Sawa et al. (2007).

For the period September to November, the ^{222}Rn concentration values associated with the maritime air masses were usually found to be less than 0.1 Bq m^{-3}, which is below the detection limit of our analyzer. However, some small ^{222}Rn peaks of 0.3 to 0.8 Bq m^{-3} can be seen in Fig. 8. These ^{222}Rn concentrations are above the detection limit of our measuring system (0.16 Bq m^{-3}) with the 32-L chamber. As was the case in December, the overall variation in ^{222}Rn corresponds well with the observed variation in CO, albeit with much smaller peaks. In fact, we find that all of the small ^{222}Rn peaks detected during the period from September to November were caused by the eastward movement of cold fronts from the Asian continent to the station. Thus, the field observation at Minamitorishima in 2007 clearly demonstrates that our new ^{222}Rn measuring system can be used for monitoring very small signals of continental influence at remote sites.

5. Conclusions and future studies

We have developed a new compact electrostatic ^{222}Rn measuring system and examined its performance by carrying out laboratory tests and field observations. From a series of laboratory tests, it was found that our new system, which uses a PIN photodiode detector for optimizing the detection limit, can carry out atmospheric ^{222}Rn measurements with greater sensitivity and higher time resolution when compared to other ^{222}Rn measuring systems that employ a similar electrostatic collection method. Furthermore, our system is very compact and has the flexibility of accommodating chambers of different sizes, making it ideal for usage in field observations. From continuous measurements at Tsukuba, we obtained half-hourly ^{222}Rn data and demonstrated that our new ^{222}Rn measuring system can capture the diurnal variation in atmospheric ^{222}Rn occurring within the surface boundary layer. The results from continuous measurements at Minamitorishima showed that our system can successfully detect very small enhanced ^{222}Rn peaks indicative of signals from the Asian continent. These results from our study show that our new ^{222}Rn measuring system is capable of resolving rapid diurnal variations and of detecting long-range transport of continental air pollution at remote sites. An establishment of a ^{222}Rn measurement network consisting of stations along the coastline of eastern Asia and at remote locations in the western North Pacific will greatly enhance our understanding of the mechanisms related to the eastward transport of pollution from the Asian continent.

We also believe that high time-resolution ^{222}Rn measurements, which can be carried out by using our instrument, will be useful in identifying the processes by which CO_2 inside a forest canopy over a complex terrain is distributed with time. For example, simultaneous measurements of ^{222}Rn and CO_2 have effectively been used for estimating the influence of nighttime drainage flows of CO_2 along the slope on the CO_2 flux measured by employing an eddy covariance method at a mountainous deciduous forest site in central Japan (Murayama et al. 2009). This will contribute to the reduction of uncertainty in the estimation of NEE under stable nighttime conditions, as pointed out by many researchers (e.g., Aubinet et al. 2005).

Acknowledgements

We would like to acknowledge Drs. Tasaka, Iida, and Moriizumi for technical suggestions and help with the calibration of the analyzer. We also thank the staff members at the Minamitorishima Meteorological Observatory of the Japan Meteorological Agency for carrying out maintenance work on the measuring system. We thank Dr. Sugawara for providing the microwave temperature profiler data. We also thank Dr. Higuchi for helpful comments and discussions. We are grateful to Mr. Kudo for his skillful help in the design and manufacturing of the ^{222}Rn analyzer. We also thank the anonymous reviewers for their valuable comments on this manuscript. This work was supported by KAKENHI17201009 (a Grant-in-Aid for Scientific Research (A)) of the Ministry of Education, Culture, Sports, Sciences, and Technology (MEXT), Japan.

References

Aubinet, A., P. Berbigier, C. H. Bernhofer, A. Cescatti, C. Feigenwinter, A. Granier, T. H. Grünwald, K. Havrankova, B. Heinesch, B. Longdoz, B. Marcolla, L. Montagnani, and P. Sedlak, 2005: Comparing CO_2 storage and advection conditions at

night at different CARBOEUROFLUX sites. *Bound. Layer Meteor.*, **116**, 63–94.

Biraud, S., P. Ciais, M. Ramonet, P. Simmonds, V. Kazan, P. Monfray, S. O'Doherty, T. G. Spain, and S. G. Jennings, 2000: European greenhouse gas emissions estimated from continuous atmospheric measurements and radon 222 at Mace Head, Ireland. *J. Geophys. Res.*, **105 (D1)**, 1351–1366.

Brunke, E.-G., C. Labuschagne, B. Parker, D. van der Spuy, and S. Whittlestone, 2002: Cape Point GAW Station ^{222}Rn detector: factors affecting sensitivity and accuracy. *Atmos. Environ.*, **36 (13)**, 2257–2262.

Budnitz, R. J., 1974: Radon-222 and its daughters—A review of instrumentation for occupational and environmental monitoring. *Health Phys.*, **26**, 145–164.

Busigin, A., A. W. Van der Vooren, J. C. Babcock, and C. R. Phillips, 1981: The nature of unattached RaA (^{218}Po) particles. *Health Phys.*, **40**, 333–343.

Chevillard, A., P. Ciais, U. Karstens, M. Heimann, M. Schmidt, I. Levin, D. Jacob, R. Podzun, V. Kazan, H. Sartorius, and E. Weingartner, 2002: Transport of ^{222}Rn using the regional model REMO: a detailed comparison with measurements over Europe. *Tellus*, **54B**, 850–871.

Chu, K. D., and P. K. Hopke, 1988: Neutralization kinetics for polonium-218. *Environ. Sci. Technol.*, **22**, 711–717.

Conen, F., A. Neftel, M. Schmid, and B. E. Lehmann, 2002: $N_2O/^{222}$Rn—soil flux calibration in the stable nocturnal surface layer. *Geophys. Res. Lett.*, **29 (2)**, 1025, doi:10.1029/2001GL013429.

Conen, F., and L. B. Robertson, 2002: Latitudinal distribution of radon-222 flux from continents. *Tellus*, **54B**, 127–133.

Currie, L. A., 1968: Limits for qualitative detection and quantitative determination Application to radiochemistry. *Analytical Chemistry*, **40 (3)**, 586–593.

Dua, S. K., P. Kotrappa, and P. C. Gupta, 1983: Influence of relative humidity on the charged fraction of decay products of radon and thoron. *Health Phys.*, **45**, 152.

Dula, G., and G. A. Dalu, 1971: An automatic counter for direct measurements of radon concentration. *J. Aerosol. Sci.*, **2**, 247–255.

Gupta, M., A. R. Douglass, S. R. Kawa, and S. Pawson, 2004: Use of radon for evaluation of atmospheric transport models: sensitivity to emissions. *Tellus*, **56B**, 404–412. DOI: 10.1111/j.1600-0889.2004.00124.x.

Hopke, P. K., 1989: Use of electrostatic collection of ^{218}Po for measuring Rn. *Health Phys.*, **57**, 39–42.

Iida, T., Y. Ikebe, and K. Tojo, 1991: An electrostatic radon monitor for measurements of environmental radon. *Res. Lett. Atmos. Electr.*, **11**, 55–59.

Iida, T., Y. Ikebe, K. Suzuki, K. Ueno, Z. Wang, and Y. Jin, 1996: Continuous measurements of outdoor radon concentrations at various locations in East Asia. *Environ. Int.*, **22**, 139–147.

Iimoto, T., Y. Shirakata, S. Tokonami, M. Furukawa, and R. Kurosawa, 1998: Continuous ^{220}Rn concentration monitor using an electrostatic collection method. *Radiat. Prot. Dosim.*, **77**, 185–190.

Jacob, D., et al., 1997: Evaluation and intercomparison of global atmospheric transport models using ^{222}Rn and other short-lived tracers. *J. Geophys. Res.*, **102 (D5)**, 5953–5970.

Josse, B., P. Simon, and V-H. Peuch, 2004: Radon global simulations with the multiscale chemistry and transport model MOCAGE. *Tellus*, **56B**, 339–356.

Kotrappa, P., S. K. Dua, P. C. Gupta, and Y. S. Mayya, 1981: Electret: A new tool for measuring concentrations of radon and thoron in air. *Health Phys.*, **41**, 35–46.

Levin, I., H. Glatzel-Mattheier, T. Marik, M. Cuntz, M. Schmidt, and D. E. Worthy, 1999: Verification of German methane emission inventories and their recent changes based on atmospheric observations. *J. Geophys. Res.*, **104 (D3)**, 3447–3456.

Li, Y., and J. Chang, 1996: A three-dimensional global episodic tracer transport model 1. Evaluation of its transport processes by radon 222 simulations. *J. Geophys. Res.*, **101 (D20)**, 25 931–25 947.

Lucas, H. F., 1957: Improved low-level alpha-scintillation counter for radon. *Rev. Sci. Instrum.*, **28**, 680–683.

Martens, C. S., T. J. Shay, H. P. Mendlovitz, D. M. Matross, S. R. Saleska, S. C. Wofsy, W. S. Woodward, M. C. Menton, J. M. S. De Moura, P. M. Crill, O. L. L. De Moraes, and R. L. Lima, 2004: Radon fluxes in tropical forest ecosystems of Brazilian Amazonia: night-time CO_2 net ecosystem exchange derived from radon and eddy covariance methods. *Global Change Biology*, **10**, 618–629, 10.1111/j.1529-8817.2003.00764.x.

Rasch, P. J., et al., 2000: A comparison of scavenging and deposition processes in global models: results from the WCRP Cambridge workshop of 1995. *Tellus*, **52B**, 1025–1056.

Murayama, S., H. Kondo, N. Saigusa, A. Wada, K. Ishijima, H. Matsueda, and Y. Sawa, 2009: Transportation of CO_2 in a mountainous cool temperate deciduous forest in central Japan estimate from atmospheric ^{222}Rn measurement. *Extended Abstract of ICDC8*, T2-051, CD-ROM.

Sawa, Y., H. Tanimoto, S. Yonemura, H. Matsueda, A. Wada, S. Taguchi, T. Hayasaka, H. Tsuruta, Y. Tohjima, H. Mukai, N. Kikuchi, S. Katagiri, and K. Tsuboi, 2007: Widespread pollution events of carbon monoxide observed over the western North Pacific during the East Asian Regional Experiment (EAREX) 2005 campaign. *J. Geophys. Res.*, **112**, D22S26, doi:10.1029/2006JD008055.

Schmidt, M., R. Graul, H. Sartorius, and I. Levin, 1996: Carbon dioxide and methane in continental Europe: a climatology, and ^{222}Radon-based emission estimates. *Tellus*, **48B**, 457–473.

Schmidt, M., H. Glatzel-Mattheier, H. Sartorius, D. E. Worthy, and I. Levin, 2001: Western European N_2O emissions—a top down approach based on atmospheric observations. *J. Geophys. Res.*, **106 (D6)**, 5507–5516.

Schmidt, M., R. Graul, H. Sartorius, and I. Levin, 2003: The Schauinsland CO_2 record: 30 years of continental observations and their implications for the variability of the European CO_2 budget. *J. Geophys. Res.*, **108 (D19)**, 4619, doi:10.1029/2002JD003085.

Stockwell, D. Z., and M. P. Chipperfield, 1999: A tropospheric chemical transport model: Development and validation of the model transport schemes. *Quart. J. Roy. Meteor. Soc.*, **125**, 1747–1783.

Taguchi, S., T. Iida, and J. Moriizumi, 2002: Evaluation of the atmospheric transport model NIRE-CTM-96 by using measured radon-222 concentrations. *Tellus*, **54B**, 250–268.

Thomas, J. W., and P. C. LeClare, 1970: A study of the two-filter method for radon-222. *Health Phys.*, **18**, 113–122.

Tokonami, S., T. Iimoto, T. Ichiji, K. Fujitaka, and R. Kurosawa, 19996: Continuous Radon monitor using a two-filter method. *Radiat. Prot. Dosim.*, **63**, 123–126.

Trumbore, S. E., M. Keller, S. C. Wofsy, and J. M. Da Costa, 1990: Measurement of soil and canopy exchange rates in he Amazon rain forest using ^{222}Rn. *J. Geophys. Res.*, **95 (D10)**, 16 865–16 873.

Ui, H., S. Tasaka, M. Hayashi, K. Osada, and Y. Iwasaka, 1998: Preliminary results from radon observation at Syowa Station, Antarctica during 1996. *Polar Meteorol. Glaciol.*, **12**, 112–123.

Wada, A., Y. Sawa, H. Matsueda, S. Taguchi, S. Murayama, S. Okubo, and Y. Tsutsumi, 2007: Influence of Continental Air Mass Transport on Atmospheric CO_2 in the Western North Pacific. *J. Geophys. Res.*, **112**, D07311(1-12), doi:10.1029/2006JD007552.

Whittlestone, S., 1985: A high-sensitivity Rn detector incorporating a particle generator. *Health Phys.*, **49**, 847–852.

Whittlestone, S., and W. Zahorowski, 1998: Baseline radon detectors for shipboard use: Development and deployment in the First Aerosol Characterization Experiment (ACE 1). *J. Geophys. Res.*, **103 (D13)**, 16 743–16 751.

Wilkening, M. H., and W. E. Clements, 1975: Radon-222 from the ocean surface. *J. Geophys. Res.*, **80**, 3828–3830.

Wrenn, M. E., H. Spitz, and N. Conen, 1975: Design of a continuous digital-output environmental radon monitor. *IEEE Trans. Nucl. Sci.*, **22**, 645–648.

Zahorowski, W., and S. Whittlestone, 1996: A fast portable emanometer for field measurement of radon and thoron flux. *Radiat. Prot. Dosimetry*, **67**, 109–120.

Zahorowski, W., S. Chambers, and A. Henderson-Sellers, 2004: Ground based radon-222 observations and their application to atmospheric studies. *J. Environ. Radioact.*, **76**, 3–33.